DR. MIRIAM S NOKIA (Orcid ID : 0000-0003-2222-6118)

Article type : Research Report

Section: Developmental Neuroscience & Neurosystems (editor: Ying-Shing Chan)

Irradiation of the head reduces adult hippocampal neurogenesis and impairs spatial memory, but leaves overall health intact in rats

Running title: Head irradiation, health and hippocampus

Sanna Lensu[1,2*], Tomi Waselius[2], Elina Mäkinen[1], Heikki Kettunen[3], Ari Virtanen[3], Marja Tiirola[4], Markku Penttonen[2], Satu Pekkala and Miriam S. Nokia[2*#]

[1] Faculty of Sport and Health Sciences, University of Jyvaskyla, Jyvaskyla, Finland

[2] Department of Psychology, University of Jyvaskyla, Jyvaskyla, Finland

[3] Department of Physics, University of Jyvaskyla, Jyvaskyla, Finland

[4] Department of Biological and Environmental Sciences, University of Jyvaskyla, Jyvaskyla, Finland

[*] authors contributed equally to this work

[#]Corresponding author: Miriam S. Nokia, miriam.nokia@jyu.fi

This manuscript consists of 46 pages of text (233 words in the Abstract, 14481 words in the whole manuscript) and 6 figures.

Keywords: adult hippocampal neurogenesis, cancer treatment, gut microbiota, inflammation, learning, *in vivo* electrophysiology

Abstract

Treatment of brain cancer, glioma, can cause cognitive impairment as a side-effect, possibly because it disrupts the integrity of the hippocampus, a structure vital for normal memory. Radiotherapy is commonly used to treat glioma, but the effects of irradiation on the brain are still poorly understood, and other biological effects have not been extensively studied. Here we exposed healthy adult male rats to small and moderate-dose irradiation of the head. We found no effect of irradiation on systemic inflammation, weight gain or gut microbiota diversity, although it increased the abundance of *Bacteroidaceae* family, namely *Bacteroides* genus in the gut microbiota. Irradiation had no effect on long-term potentiation in the CA3-CA1 synapse or endogenous hippocampal electrophysiology, but it did reduce adult hippocampal neurogenesis and impaired short-term spatial recognition memory. However, no overall cognitive impairment was observed. To summarize, our results suggest that in adult male rats head irradiation does not compromize health or cognition overall even though the number of new, adult-born hippocampal neurons is decreased. Thus, the sole effects of head irradiation on the body, brain and cognition might be less harmful than previously thought, and the cognitive decline experienced by cancer patients might originate from physiological and mental effects of the disease itself. Therefore, and to increase the translational value of animal studies, the effects of irradiation should be studied together with cancer, in older animals, using varying irradiation protocols and doses.

Introduction

Chemotherapy and irradiation used for treating cancer, especially when targeted to the head and brain in order to treat glioma, are reported to cause cognitive dysfunction in humans (Gondi et al. 2012; for review see, Lawrie et al. 2019). The harmful symptoms include decreased processing speed, executive function, attention and memory. Reports on the prevalence and severity of the impairment vary. When experienced, the cognitive deficits brought about by cancer treatment influence adherence to the treatment and can lead to long-term, clinically significant impairment that has a major impact on the quality of life (Janelsins et al. 2011; Janelsins et al. 2017). Thus, the biological basis of these difficulties has become an important target of research. Although not directly translatable to humans, studies conducted in healthy animal models can provide detailed information on the effects of cancer treatment itself on the brain both at the cellular and systems level.

It is known that the cognitive functions negatively affected by chemo- or radiotherapy in rodent models are in part dependent on the structural integrity of the hippocampus (see for example Nokia et al. 2012; Lacefield et al. 2012; Park et al. 2015; Winocur et al. 2015). Hippocampus is thought to be crucial for the formation of episodic memories (Scoville and Milner 1957) and for the accurate processing of both spatial (O'Keefe and Dostrovsky 1971) and temporal information (Pastalkova et al. 2008; MacDonald et al. 2011; Mau et al. 2018). New neurons are continuosly produced through a process called adult hippocampal neurogenesis (AHN, for review see Toda and Gage 2018). At the moment, it is still unclear whether and to what degree adult neurogenesis takes place in the human hippocampus (see for example Lucassen et al., 2020; Petrik and Encinas, 2019) but for now this possibility is considered viable. In the rodent brain, AHN results in new granule cells in the dentate gyrus of the hippocampus. These cells are thought to be important for pattern separation (Clelland et al. 2009; Sahay et al. 2011; Neunuebel and Knierim 2014; Franca et al. 2017; Winocur et al. 2006), cognitive flexibility (Burghardt et al. 2012; Anacker et al. 2018), and associative learning (Shors et al. 2001; Nokia et al. 2012; Seo et al. 2015; Miller et al. 2019; for a recent review on AHN and memory, see Miller and Sahay 2019). Irradiation (Monje et al. 2002) and chemotherapy (Shors et al. 2001; Nokia et al. 2012) both reduce AHN. Thus, cancer treatment can cause changes in hippocampal structure, diminishing its capacity for plasticity that might partly also explain the specific impairments in cognition.

To further probe the causes for cancer treatment-related cognitive decline, studies in rodent models have considered the effects of irradiation and chemotherapy on hippocampal electrophysiological function. In healthy adult rodents, hippocampal electrophysiology is characterized by regular theta (3-8 Hz) (Buzsáki 2002) and gamma (30-80 Hz) oscillations (Colgin 2016), as well as intermittently occurring dentate spikes (duration 20-50 ms, amplitude ~0.5-2 mV) (Bragin et al. 1995; Penttonen et al. 1997; Headley et al. 2017) in the dentate gyrus and sharp-wave ripples (SPW-Rs, Buzsáki 2015) in the CA1 region. All these phenomena are important for learning and memory: theta and gamma for the initial encoding and SPW-Rs and dentate spikes for consolidation of new memory traces (theta and gamma: Colgin 2016, dentate spikes: Nokia et al. 2017; Lensu et al. 2019, SPW-Rs: Buzsáki 2015). Studies suggest that irradiation of the head and subsequent decrease in AHN elevates endogenous dentate gyrus excitability at the gamma band (Lacefield et al. 2012; Park et al. 2015, see also Ikrar et al. 2013) while attenuating theta oscillations (Park et al. 2015, see also Nokia et al. 2012). Irradiation of the head is also reported to decrease dentate gyrus responses to electrical stimulation of the perforant path (Lacefield et al. 2012; Park et al. 2015), the major input stream from the entorhinal cortex to the hippocampus. In addition, irradiation and the resulting decrease in AHN is reported to impair long-term potentiation at the perforant path to dentate gyrus synapse (Saxe et al. 2006; Snyder et al. 2001; see also Singer et al. 2011). Silencing adult-born neurons might increase contralateral hippocampal CA1 excitability at a broad frequency band (15-100 Hz, Zhuo et al. 2016). However, it is not known if and how irradiation affects, for example, dentate spikes (Nokia et al. 2017; Lensu et al. 2019) or long-term depression in the dentate gyrus. To conclude, knowledge on the effects of head irradiation and subsequent reduction in AHN on hippocampal electrophysiology is still incomplete.

In addition to the tissues directly targeted, radiotherapy can also have an impact on peripheral organs, either directly or via, for example, systemic inflammation (Gandhi and Chandna 2017). One of the organs possibly affected is the gut and the composition of its inhabitants, the gut microbiota. Gut microbiota refers to the trillions of gut-inhabiting microbial organisms, which according to the current knowledge can affect brain function in several ways (for recent review, see Cryan et al. 2020). Emerging evidence suggests that gut-derived inflammatory cytokines can affect neurodegeneration via neuroinflammation (Lin et al. 2019). The gut and enteric nervous system located within the digestive tract are linked to the brain via both the vagus nerve and several direct and indirect molecular pathways, together termed the gut-brain axis (Bonaz et al.

2018). Recent studies have highlighted the importance of the gut-brain axis in regulating cognitive functions (for review, see Smith and Wissel 2019). Further, cancer patients receiving radiotherapy to body parts other than the brain, exhibit marked disturbances of the gut homeostasis and gut microbiota composition (Touchefeu et al. 2014). While it is known that head and neck cancer patients treated with radiotherapy are highly susceptible to toxic intestinal mucositis (Trotti et al. 2003), to our knowledge, the effect of brain irradiation on the gut microbiota has not been studied.

In human patients, radiotherapy consists of repeated small doses of irradiation, e.g. 1.8 – 2 Gy over several weeks resulting in total dose of 50 - 60 Gy (Lawrie et al. 2019). Here, we examined the sole effects of head irradiation, conducted either once at 8.5 Gy (Experiment 1) or twice at 10 Gy (Experiment 2) on AHN, systemic inflammation, gut microbiota diversity and composition, hippocampal electrophysiology and learning using adult male Sprague-Dawley rats as subjects. Our hypothesis was that irradiation would cause inflammation and alter gut microbiota, abolish AHN, disrupt synaptic plasticity and endogenous electrophysiological activity in the hippocampus, and thus impair learning and memory.

Materials and Methods

Ethical Approval

All the experimental procedures were approved by the Animal Experiment Board of Finland (licence nrs. ESAVI-6718-04.10.07-2015 and ESAVI-24666-2018) and implemented in accordance with directive 2010/63/EU of the European Parliament and of the Council on the care and use of animals for research purposes.

Subjects

The subjects were 40 adult male Sprague-Dawley rats purchased from a commercial vendor (Envigo, Netherlands). Animals for Experiment 1 arrived at the age of seven weeks and for Experiment 2 at the age of 4 weeks. Note that for Experiment 2 we used slightly younger animals to emphasize the effects of irradiation on AHN – it is known that neurogenesis in the hippocampus declines rapidly with age. Also note that during irradiation, rats in both experiments were considered young adults (see Sengupta, 2013). All animals were housed in pairs on the premises of the animal research unit at the University of Jyvaskyla, Finland. Food and water were available *ad libitum*, and room temperature and humidity were controlled at 21 ± 2°C and 50 ± 10%, respectively. All rats were kept in Macrolon 1354, type IV cages (Techniplast, Buguggiate, Italy) and had aspen chips (Tapvei, Harjumaa, Estonia) at the bottom of the cage as bedding material. The rats also had a red plastic tube as a toy and shelter. The rats were maintained on a 12 h–12 h light–dark cycle, with lights on at 08.00 am. All procedures were conducted during the light portion of the cycle. Body weight and food intake were regularly followed after the irradiation.

Timeline

The timeline of the two experiments is depicted in Figure 1. Prior to the irradiation, the rats in Experiment 1 were habituated to the exploration and then trained on an object location task to obtain a baseline measure. After irradiation, the rats were subjected to a context-object - discrimination task, a fixed interval task and the object location task. For the rats in Experiment 2, we conducted a set of spatial tasks before and after the irradiation (habituation, object location task and episodic-like memory task) (please see Inostroza et al. 2013). At last, all rats were anesthetized with urethane and hippocampal electrophysiology was examined acutely *in vivo*.

After completion of the recordings, the anesthetized animals were euthanized by decapitation. Histological samples were extracted from the brain.

Irradiation

All animals were transported in ventilated cardboard boxes to the Department of Physics at University of Jyvaskyla for irradiation. Each animal was lightly anesthetized with a low dose of pentobarbital (30 mg/kg, 30 mg/ml diluted in saline, *i.p.*). Half of the animals were placed back in the transport box and served as controls. The other half were irradiated. For the irradiation, the head of the rat was fixed in a stereotaxic device using blunt earbars and the whole rat was covered with lead plates resting on support structures around the rat. There was a round hole of 1 cm in diameter, in the lead shield covering the head. The hole was aimed above the hippocampus. Varian Clinac linear accelerator was used to deliver gamma rays at a rate of 1 Gy per minute. In Experiment 1, a dose of 8.5 Gy was used. In the second experiment, a dose of 10 Gy was used and irradiation was performed on two consecutive days to obtain a total dose of 20 Gy. All in all, the irradiation procedure of one rat took ~15 min. After recovering from anesthesia (~30 min), the rats remained in the transport boxes until they were returned to the animal facilities and placed back in their respective home cages. Note that in Experiment 2, one rat in the irradiation group did not recover from anesthesia during the second day of irradiation leaving thus only nine animals to that group. In all other groups, there were ten animals.

Behavioral tasks

All of the tasks involving spatial exploration were video-recorded using an overhead webcam connected to a computer. The objects were always placed ~15 cm from the wall and from each other to ascertain that there was enough room for the rat to move. The arena and objects were cleaned between each animal and exposure using 70% ethanol solution (Experiment 1) or tap water (Experiment 2). The room was kept quiet and the lighting was provided by standard laboratory ceiling light fixtures.

Experiment 1

Habituation to exploration

To habituate the animals to the behavioral testing situation and to monitor their overall activity, we performed the open field test. The animal was placed in a 74 cm x 74 cm open arena

with 30 cm high plexiglass walls and let to freely roam there for 5 minutes. Behavior was evaluated off-line from the recorded videos by an experimenter blind to the animal identity. From the open field recordings, both movement and time spent in the center of the arena were determined. This was accomplished by dividing the arena into 16 squares of equal size and counting the number of border crossings and the time spent in the most middle four squares.

Object location task

The object location task is hippocampus-dependent and considered to measure spatial recognition memory (Barker and Warburton 2011). For this task, the same arena was used as in the open field test. Two identical objects were placed in the arena. The animal was first let to explore the objects for 5 min. Then, the rat was removed and returned to the home cage for one minute. During the delay, the arena and objects were wiped clean and one of the objects was moved to another, previously unoccupied location. Then the same animal was returned to the arena and let to explore freely for one minute. The rat was expected to pay more attention to the *object in the new location*. To qualify for inclusion in analysis the animal had to explore both objects, for a total of at least 20 s during the sample exposure. Object exploration was defined as pointing the nose towards the object within < 2 cm distance or otherwise physically interacting with the object (i.e. leaning on it, climbing over it etc.). The time spent exploring each object was scored in seconds and the percentage of time spent exploring the object of interest was calculated relative to total time spent exploring all objects. This recognition index was used as the final measure of performance.

Context-Object Discrimination (COD)

As mentioned in the introduction, dentate gyrus is thought to be crucial in forming separate representations of similar events, a process termed pattern separation (Knierim and Neunuebel 2016). Previous studies have indicated that especially adult-born hippocampal granule cells might be involved (Franca et al. 2017). The performance in the COD task relies on pattern separation and is dependent on an intact hippocampus in rats (Mumby et al. 2002). The protocol was modified from the one used by Czerniawski et al. (2015) and was similar to another used in our recent experiment indicating better pattern separation after hippocampal disruption during memory consolidation (Lensu et al. 2019).

For COD, we used two different arenas and two different pairs of identical objects in different rooms. The arena A was square-shaped, 74 cm x 74 cm, with 30 cm high, plexiglass

walls. The walls were covered with white paper from the outside. On one wall, there was a black square in the middle, on second wall a blue cross and on third, a strip of striped tape. The floor was made of clear plexiglass with a white background. Black markings divided the floor into 16 equal-size squares. The arena B was round-shaped (~74 cm diameter, 30 cm high walls) and the wall was made of matte white metal sheet. The floor of the arena B was a black rubber mat. The arenas were located in two different rooms (on opposite sides of the corridor) having a slightly different lighting and distinct furniture. The objects used were made of glass (transparent square) and stone (gray, round) candle holders (upside-down).

On two consecutive days, the rat was placed into the arenas A and B and allowed to freely explore the objects and the arena for 10 minutes. Between the arena visits 1 and 2 (Day 1) and 3 and 4 (Day 2), each rat was returned to its home cage for ~2.5 hrs. The daily sessions were conducted with an interval of ~24 hrs. The order of visits to the arenas A and B was pseudorandomized and counterbalanced. The test session took place on Day 3 and consisted of 5 min in either arena A or B (counterbalanced and pseudorandomized). During this time, one of the objects in the arena was consistent with the training (in context) but the other object was the one usually presented in the other arena (out of context). The rat was expected to pay more attention to the *object that was out of context*. The task was performed only once, two months after irradiation. Object exploration and recognition was analyzed off-line as described for the object location task above.

Fixed Interval (FI) task

In addition to the spatial tasks, we wanted to study the effects of irradiation on temporal processing. For the purpose, we used a fixed interval task. The performance in this task is known to depend on the dorsal hippocampus. Animals with lesions tend to seek for the reward too early (see for example Yin and Meck 2014).

The protocol for the FI training was similar to that used in our recent experiment related to dentate spikes and learning (Lensu et al. 2019). The animals were maintained on a restricted diet of ~15 g of food pellets per day, starting from the day prior to the first pretraining session. The training took place inside a cylinder (diameter 20 cm, height 40 cm) made of clear acrylic material in dim lighting. A white noise generator was used to create a steady background noise of ~75 dB. A nose poke port (diameter ~2 cm) was on one side of the cylinder, approximately 5 cm from the bottom. On the opposite side of the cylinder, another hole was made to deliver the reward pellet onto a black concave acrylic block (1.5 cm x 2 cm) serving as a pellet tray. The reward was

delivered using a standard pellet dispenser (ENV-203-45, Med Associates Inc. Fairfax, VT, USA) connected to the pellet tray with silicone tubing.

The experiment was controlled by an Arduino® and nosepokes were detected using two LEDs placed on opposite sides of the opening in the cylinder wall, outside the cylinder. This meant that the animal had to purposely extend its neck to break the LED beam for a reward. Only a nosepoke that took place after the target interval had elapsed, was rewarded and one 45-mg pellet was delivered at a time. First, the animals were pretrained to the procedure using a 17-second fixed interval. Two 30-minute sessions were conducted on consecutive days. Then, the actual training was started using a 143 s fixed interval. Altogether 15 sessions were conducted, one per day, on consecutive days. Each session lasted for 1 hr allowing up to 25 trials per day. The nosepokes and pellet deliveries were recorded as TTL pulses using an A/D converter (Digidata 1320A, Molecular Devices) and AxoScope (Molecular Devices) software with a 100 Hz sampling rate. The task was performed only once, two months after irradiation.

To evaluate timing performance in the FI task, the data was analyzed off-line using Matlab. First, the probability of a nose poke was determined for the first half of the fixed interval (false response) and for the period exceeding 90% of the fixed interval (correct). Then, the ratio between the correct response probability and the summed probability of both false and correct responses was calculated (0 = only false responses, 1 = only correct responses) and converted to percentage. A value of 80 % was set as a criterion for learning.

Experiment 2

The tasks were selected from a repertoire used in the study by Inostroza et al. (2013) for probing cognition in an experimental model of temporal-lobe epilepsy with abnormal hippocampal structure and function.

Habituation to exploration

The open field task was performed prior to irradiation similar to Experiment 1 but the animals were let to explore the arena for 10 minutes. The procedure was repeated three times to familiarize the rats to the arena: twice on the first day and once on the following day. The next day, we conducted the Object-Place memory task as described in Inostroza et al. (2013). The rat was let to explore two different objects placed in an open arena for 3 min, and then returned to homecage. After a ~65 min delay, the rat was again placed into the arena and let to explore for 3 min. This time, one of the two objects had been replaced by an object identical to the one, which

was left untouched. Thus, there were now two identical objects in the arena occupying the same locations as before. Two months after the irradiation, the habituation to exploration was performed by subjecting the animals to the Object-Place memory task only. Note that in a previous study by Inostroza and colleagues, the performance in the Object-Place memory task was unaffected by temporal-lobe epilepsy and associated hippocampal abnormality (Inostroza et al. 2013). For the purpose, we used new objects in a different arena and room. Note that we do not report results for the Object-Place task used for habituation, as animals spent minimal time exploring the objects and no reliable measures were thus obtained for most rats.

Object location task

The protocol for this hippocampus-dependent task was similar to the one used in Experiment 1, except that the delay between explorations was longer (1 min vs. 65 min) to conform with the delay used in the study by Inostroza et al. (2013). Two novel, identical objects were placed in the arena. The animal was first let to explore the objects for 3 min. Then, the rat was removed and placed in the home cage for ~65 minutes. During the delay, the arena and objects were wiped clean and one of the objects moved to another, previously unoccupied location. Then, the same animal was returned to the arena and let to explore freely for 3 minutes. The rat was expected to pay more attention to the *object in the new location*. The task was performed prior to and two months after irradiation and data analyzed as in Experiment 1 with the exception that a shorter period of exploration (5 s vs. 20 s in Exp. 1) was used as the inclusion criterion, due to the fact that the animal was allowed a shorter time periof for exploring overall (3 min compared to 5 min in Exp. 1).

Episodic-like memory task

For examining the effects of irradiation on episodic-like memory, we used a task described earlier to discriminate rats with impaired hippocampal structure and function from normal rats (Kart-Teke et al. 2006; Inostroza et al. 2011; Inostroza et al. 2013). In the first exploration, four identical objects were placed in the arena and the rat was let to explore for 3 min. After spending ~65 min in the homecage, the rat was again placed in the same arena for 3 min, but this time a different set of four identical objects was displayed. Two of the objects were in the same location as those presented earlier, and two in previously unoccupied locations. After another ~65 min delay in the homecage, the rat was let to explore the arena one final time for 3 min. Now, two objects from each set were presented: One from the first set in its original place (A1, remote

stationary), one from the first set in a location previously occupied by another object from the latter set (A2, remote displaced), one from the latter set in its original location (B1, recent stationary), and one from the latter set in a location previously occupied by another object from the first set (B2, recent discplaced). The rat was expected to pay more attention to the stationary remote object (A1) and to the displaced recent object (B2) (Kart-Teke et al. 2006; Inostroza et al. 2013). The task was performed prior to and 2 months after the irradiation.

Object exploration was analyzed off-line as described above for the object location task. In the episodic-like memory task where four objects were presented at once, we calculated a "Where" index ([B2 - B1] / [B2 + B1]) and a "When" index ([A1 - B1] / [A1 + B1]) (Inostroza et al. 2013). These indexes are close to zero if the rat shows no preference and explores all objects at a chance level. If the index is positive, the rat preferred to explore the recently displaced object (B2, "where") or the old stationary object (A1, "when"). If the index is negative, the rat preferred to explore the recent stationary object (B1).

Hippocampal electrophysiology

Surgery

After the completion of cognitive tests, the animals were anesthetized with urethane (1.3–1.5 g/kg, 0.24 g/ml, *i.p.*, Sigma-Aldrich, St. Louis, MO, US). The head of the animal was attached to a stereotaxic instrument (David Kopf Instruments, Model 962, Tujunga, CA, US). Under local anaesthesia (bupivacaine, 2 mg, 2.5 mg/ml, *s.c.*), the skin was removed, and a craniotomy was made above the hippocampus (3.6 to 4 mm posterior and 1.1 to 2.2 mm lateral to the bregma). A silicon probe (Atlas Neurogengineering, E32-65-S1-L6-NT) with a linear configuration of 32 electrodes, 65 microns apart was implanted to the dorsal hippocampus, targeting the tip at the lower blade of the dentate gyrus (~4 mm below dura). A 27 G injection needle (Terumo, Leuven, Belgium) inserted to the cerebellum served as the reference and ground. In Experiment 1, a bipolar stimulation electrode was implanted into the angular bundle ipsilateral to the recording electrode for perforant path stimulation at 7 mm posterior and 3.5 mm lateral to the bregma, ~3.2 mm below dura. In Experiment 2, the stimulation electrode was implanted to the contralateral ventral hippocampal commissure at 1.3 to 2 mm posterior, ~1 mm lateral to bregma and ~4.0 mm below dura. In both cases, the stimulation electrode was made of Formwar-coated stainless steel dual-wire with a diameter of 100 μm and a tip separation of ~500 μm. Electrode depths were based on

on-line visual detection of sharp-wave ripples, theta, gamma and dentate spikes and responses to stimulation.

Recording

All data was band-pass filtered between 1 and 5000 Hz and stored at a 20 kHz sampling rate using Multichannel Systems (MCS, Reutlingen, Germany) equipment (a modified 4x μPA32 connected to a FA64I and finally to a USB-ME64 unit). Stimulations were delivered by an 8-ch programmable stimulator (STG4008, MCS).

The recording always started with 30 minutes of baseline local-field potentials (LFPs) during which no stimulation was implemented. This data was used for analyzing spontaneous hippocampal activity. Then, an input-output curve was obtained for the stimulation by delivering two consecutive sets of rising and falling series of stimulations using sets of five 200-μs bipolar pulses of increasing/decreasing amplitude (20, 40, 60, 80, 100, 120, 140 and 160 μA) delivered at a 5 s interval. Based on the responses in the target area, the amplitudes used for baseline stimulation and that used for low-frequency stimulation (Experiment 1) or theta burst stimulation (Experiment 2) were selected. The baseline stimulus was set at the lowest amplitude that evoked a stable, ~0.5 mV response every time.

Experiment 1. Long-term depression

The stimulation electrode was placed in the angular bundle and the recording probe in the ipsilateral dorsal hippocampus. For inducing long-term depression in the perforant path to dentate gyrus synapse, the low-frequency stimulation amplitude was set at around ~95 % of the amplitude needed to evoke maximal responses in hilus. In practice, the baseline stimulus was 20-80 μA and the low-frequency stimulus was 140-150 μA in amplitude. At first, a 30-min baseline recording for stimulation responses was conducted. The baseline stimulus was delivered every 30 s. Then, low-frequency stimulation was conducted comprising of 900 bipolar pulses at a rate of 1 Hz (= 15 min). After that, to test the effects of low-frequency stimulation, the responses to the baseline stimulus (single pulse every 30 s) were recorded for 60 minutes.

Experiment 2. Long-term potentiation

The stimulation electrode was placed in the ventral hippocampal commissura and the recording probe in the contralateral dorsal hippocampus. For inducing long-term potentiation in the CA3-CA1 synapse, the theta-burst stimulus amplitude was set at around ~95% of the amplitude needed to evoke maximal responses in CA1. In practice, the baseline stimulus was 20-

80 µA and the theta-burst stimulus was 140-150 µA in amplitude. Next, a 30-min baseline recording for stimulation responses was conducted. The baseline stimulus was delivered every 30 s. Then, theta-burst stimulation was conducted as follows: A bipolar 200-µs pulse was repeated 4 times at an interval of 10 ms (= 100 Hz). These bursts were repeated 8 times with an interval of 200 ms (= 5 Hz). This block was repeated 4 times at an interval of 20 seconds. That is, altogether (4 x 8 x 4 =) 128 stimulation pulses were applied. Finally, to test the effects of theta-burst stimulation, responses to the baseline stimulus (a bipolar pulse every 30 s) were recorded for 60 minutes.

Histology for electrode locations

After the electrophysiological recordings, while under deep urethane anesthesia the rats were killed by rapid decapitation using a guillotine. The brain was extracted and fixed in 4% paraformaldehyde solution (pH 7.4) for at least 48 h. Then, it was stored in 0.1M phosphate buffered saline and coronally sectioned with a vibratome (Leica VT1000) into 40 µm slices. Slices with electrode marks in the hippocampus were attached to slides, dried and then stained with Prussian blue and Cresyl violet. The electrode locations were determined with the aid of a light microscope and a brain atlas (Paxinos 1998).

Electrophysiology data analysis

All analyses were performed off-line using custom made scripts in Matlab. From the baseline LFPs, signals originating in the CA1 pyramidal cell layer, the molecular layer and hilus were determined. First, Fast Fourier Transforms (FFTs) from each of these signals were calculated using the 'pwelch' command in Matlab. For visualization, the FFT result of each animal was normalized by dividing all power values by the mean of the power at all frequencies. Next, SPW-Rs (120–230 Hz), theta (3–8 Hz), gamma (25–80 Hz), high gamma (80–140 Hz) and dentate spikes were identified. SPW-Rs were detected based on the band-pass filtered signal originating in the CA1 pyramidal layer using a threshold of mean (M) + 7 * standard deviation (SD). To qualify, the ripple had to exceed the threshold at least for 20 ms. The theta epochs were detected from the molecular layer signal based on the relative power of the theta oscillation compared to combined power of all slow oscillations (3.4–8.2 Hz / 0.5–20 Hz). An epoch was considered theta epoch if the ratio was above 80. Gamma and high gamma epochs were detected from band-pass filtered signal originating in the hilus. Gamma and high gamma epochs were identified as 500-ms periods during which the said activity exceeded a threshold of M + 2.5 *SD. For visualization and further

analysis, SPW-Rs, theta, gamma and high gamma epochs were aligned based on the phase of the oscillation. This was derived from the band-pass filtered signal by means of first calculating the Hilbert-transform and the using the angle-function in Matlab. The dentate spikes were detected using simple thresholding as before (Nokia et al. 2017). Briefly, the hilar LFP signal was monitored using two consecutive sliding 10-ms windows. To qualify as a dentate spike, the signal had to increase in amplitude from one window to another by a value greater than the M + 4 * SD of the raw LFP. Dentate spikes were aligned based on the peak for further analysis. From all suitable epochs we then calculated a current source density map and plotted that together with the averaged LFPs to visualize the data for each event. Finally, the rate per minute, peak amplitude (μV) and slope (μV/ms) of the dentate spikes was determined and compared between groups. Also the amplitude of gamma and high-gamma epochs in the hilus was determined and compared between groups.

Experiment 1. Long-term depression

To determine the responses to the perforant path stimulation, current-source density analysis was performed on the LFPs recorded with a linear probe. The result corresponds to the unscaled second derivate of the potential for each recording depth. From these signals, the one indicating a current sink in response to the perforant path stimulation was used to calculate response slope (mV/s). Then, response slopes were divided by the mean of the response slope during the baseline stimulation period (30 min, 60 stimuli) and multiplied by 100. This relative measure was used to study possible effects of low-frequency stimulation.

Experiment 2. Long-term potentiation

To determine the responses to the ventral hippocampal commissure stimulation, current-source density analysis was performed on the LFPs recorded with a linear probe. Based on the current source density signals and the evoked potentials, the signal corresponding to the CA1 pyramidal cell layer was identified. Response slopes were derived from the selected LFP signal (mV/s). Then, response slopes were divided by the mean of the response slope during the baseline stimulation period (30 min, 60 stimuli) and multiplied by 100. This relative measure was used to study possible effects of theta-burst stimulation.

Adult hippocampal neurogenesis

To quantify AHN, we performed immunohistochemical staining for doublecortin on free-floating sections throughout the hippocampus as previously described (Nokia et al. 2016). Briefly, during sectioning, every 12th hippocampal section was collected into a tube filled with cryoprotectant solution (30% sucrose + 30% ethylene glycol in 0.1 M phosphate buffer, pH 7.6). The samples were stored at -20°C until staining with-doublecortin primary antibody (1:250, goat ab, sc-8066, Santa Cruz Biotehnology Inc., Texas, USA). Staining was visualized using secondary antibody biotinylated rabbit anti-goat IgG (1:1000, BA-5000, Vector Labs, Burlingame, California, USA), tertiary antibody Strepavidin-horseradish peroxidase conjugate (1:1000, RPN1231, GE Healthcare, Chalfont St Giles, Buckinghamshire, UK) and finally color was developed with diaminobenzidine (2.5 mg/ml). Negative controls were stained without primary antibody and corfirmed to have no staining. The number of doublecortin-labelled cells in the granule cell layer and the hilus were counted under a light microscope (Leica VT1000 microscope, Olympus UPlanFLN objective, 40x/NA 0.75) from a total of up to nine slices, 6.3–1.8 mm posterior to bregma (Paxinos 1998). The number of cells was multiplied by 24 to obtain an estimate of the total number of labelled cells in both hippocampi.

Gut microbiota

Fecal samples were collected and immediately snap-frozen in liquid nitrogen, five weeks after irradiation from awake rats (Serbanescu et al. 2019). Samples were stored at -80°C. The DNA was extracted from ~80 mg of the feces with Stool Extraction Kit and semi-automated GenoXtract (Hain Lifescience GmbH, Nehren, Germany), combined with an additional homogenization using bead-beating in 1.4 mm Ceramic Bead Tubes.

For the microbial community analysis, rRNA gene was amplified using primers 515F-Y (GTGYCAGCMGCCGCGGTAA) and 806R (GGACTACHVGGGTWTCTAAT) targeting the V4 region of the SSU rRNA gene. In the first PCR, the reaction consisted of 1xMaxima™ SYBR Green qPCR Master Mix (Thermo Fisher Scientific, Waltham, MA, USA), 0.25 μM of primers and ~20 ng of DNA template. Thermal cycling consisted of 10 min initial denaturation at 95°C, 30 cycles at 95°C 30 sec, +50°C 60 s and 72°C 60 s and final extension at 72°C for 10 min (C1000 ThermalCycler, Bio-Rad Laboratories, Hercules, CA, USA). To add Ion Torrent PGM sequencing adapters and barcodes to the ends of the PCR product, one μl of the PCR product was used as template in the second PCR, where 10 cycles were performed using linker and fusion primers

(0.05 µM of M13_515F-Y, 0.5 µM of IonA_IonXpressBarcode_M13 and 0.5 µM P1_806R), with conditions otherwise identical to the first amplification. Sequencing was performed using Ion Torrent PGM (Thermo Fisher Scientific). PCR products were purified with AMPure XP (Beckman Coulter, Brea, CA, USA), quantified with PicoGreen (Quant-iT™ PicoGreen™ dsDNA Assay Kit, Thermo Fisher Scientific), and pooled in equimolar quantities for sequencing on Ion Torrent PGM using Hi-Q View OT2 Kit for emulsion PCR, Hi-Q View Sequencing Kit for the sequencing reaction, and Ion 318 Chip v2 (Thermo Fisher Scientific). The 16S rRNA gene sequences were trimmed to a minumum length of 200 basepairs, quality filtered and clustered to operational taxonomic units (OTUs) at the 97% similarity using CLC Microbial Genomics Package (Qiagen, Hilden, Germany). OTUs with an abundance lower than 20 and relative abundance lower than 0.05 % were filtered out. After processing, the data-set contained 1.16 million reads, on average 60877 ± 19739 reads per sample and 12565 unique OTUs. For calculating diversity indexes, the data was further subsampled to 16539 reads per sample. The rRNA gene sequences were classified using SILVA SSU Ref database (v132, 99%).

Systemic inflammatory cytokines

Serum was separated from the whole blood samples collected from awake rats two weeks before and five weeks after the irradiation. To analyze systemic inflammation in serum, Quansys 9-plex cytokine ELISA-kit #110449RT and Q-View software (Quansys Biosciences, Logan, UT, USA) were used according to the manufacturer's instructions. The limits for the detection of cytokines were as follows; Interleukin (IL)1α 6.87 pg/ml, IL1β 1.17 pg/ml, IL2 4.9 pg/ml, IL4 2.05 pg/ml, IL6 15.57 pg/ml, IL10 2.74 pg/ml, IL12 0.41 pg/ml, Interferon-γ (IFNγ) 30.04 pg/ml, Tumor necrosis factor-α (TNFα) 14.4 pg/ml.

Statistics

The statistical analyses of the gut microbiota composition and diversity were performed using CLC Microbial Genomics software package (Qiagen). The alpha-diversity (*i.e*. species richness, distribution of evenness between species) of the gut microbiota was quantified with Shannon index and the group differences were compared using Kruskall-Wallis test. Beta-diversity (*i.e.* difference in taxonomic abundance profiles) analysis was based on Bray-Curtis distance, Weighted unifrac and PERMANOVA. The taxonomic groups were compared based on Analysis of variance (ANOVA) -like analysis across groups, followed by Benjamini-Hochberg

correction for multiple testing. The statistical significance was set at $p < 0.05$ after the multiple testing correction.

All other analyses were performed with IBM SPSS Statistics 26 (IBM Corporation, Armonk, NY, USA) or SigmaPlot 12.5 (Systat Software Inc. San Jose, CA, USA). ANOVA and t-tests were used for comparisons. Bonferroni-correction was used for post-hoc tests. Greenhouse-Geisser corrected p-values are reported in cases where the sphericity assumption was violated. The statistical significance was set at $p < 0.05$.

Results

Irradiation of the head had no adverse effect on overall health but significantly reduced adult hippocampal neurogenesis

We started by analyzing possible systemic effects of irradiation to the head. The simplest measure for this is body weight (Figure 1C). Irradiation had no effect on weight gain in Experiment 1 (repeated measures [rm] ANOVA: main effect of time: $F [1, 18] = 886.82$, $p < 0.001$, main effect of treatment: $F [1, 18] = 0.12$, $p = 0.736$, interaction of time and treatment: $F [1, 18] = 0.33$, $p = 0.573$) nor in Experiment 2 (rm ANOVA: main effect of time: $F [1, 17] = 735.03$, $p < 0.001$, main effect of treatment: $F [1, 17] = 0.13$, $p = 0.726$, interaction of time and treatment: $F [1, 17] = 0.10$, $p = 0.761$). In Experiment 2, we also retrieved blood samples from the rats two weeks prior and five weeks after the irradiation. At both time points, and in both irradiated and control rats, the level of eight inflammatory cytokines (see Materials and Methods) was under the detection limit. The only detected cytokine, IL12, tended to be higher in the controls compared to irradiated rats prior to irradiation (rm ANOVA: interaction of time and treatment: $F [1, 17] = 5.32$, $p = 0.034$; rm ANOVA, Ctrl: $F [1, 9] = 10.22$, $p = 0.011$; 2 x 10 Gy: $F [1, 8] = 0.17$, $p = 0.692$), but the differences between groups did not reach statistical significance either before or after the irradiation (one-way ANOVA: pre-irradiation: $F [1, 17] = 3.47$, $p = 0.080$; post-irradiation: $F [1, 17] = 0.00$, $p = 0.973$) (Figure 2A).

We also analyzed the gut microbiota from feces of both control and irradiated (2 x 10 Gy, Experiment 2) rats at five weeks post-irradiation. Irradiation had no effect on the distribution of species *i.e.* the alpha-diversity of gut microbiota (Shannon index, one-way ANOVA: $F [1, 17] = 0.61$, $p = 0.444$) (Figure 2B). Similarly, PERMANOVA analysis of beta-diversity revealed no differences between irradiated and control rats in taxonomic abundance (Bray Curtis, Figure 2E, panel i) or sequence distances (Weighted UniFrac, Figure 2E, panel ii). The abundance of different microbial taxa at phylum, family and genus level in the gut is visualized in Figure 2F. Bacteroidetes (52.1% of all sequences) and Firmicutes (45.3%) were the dominating bacterial phyla, followed by Actinobacteria (0.06%) and Proteobacteria (0.05%). Families Muribaculaceae (32.8%, only genus *Muribaculum*) and Rikennellaceae (13.6%, only genus *Alistipes*) explained the dominance of Bacteroidetes, and families Ruminococcaceae (20.3%), Lachnospiraceae (10.9%) were dominating the sequences belonging to Firmicutes.The gut microbiota composition did not differ between the groups at phylum level (Figure 2F, panel i). The average composition at family

and genus level in the groups are shown in Figure 2F panel ii) and iii). At family level differences were found in the relative abundance of family Bacteroidaceae and further the genus *Bacteroides* (one-way ANOVA, F [1, 17] = 5.09, p = 0.038 and corrected p = 0.044 for both) (Figure 2C and 2D). To conclude, irradiation of the head had no clear adverse effects, such as effects on body weight or gut microbiota, neither did it induce systemic inflammation.

Next, we determined the effect of irradiation on AHN. The results are illustrated in Figure 3. Doublecortin was used as a marker for new, immature adult-born neurons in the DG. Irradiation at 8.5 Gy at the age of ~4.5 months in Experiment 1 reduced the number of new neurons in the dentate gyrus by ~65 %, as quantified at the age of ~8 months [independent samples t-test: t (18) = 5.88, p < 0.001] (Figure 3, A and C). Irradiation at 2 x 10 Gy at the age of ~3 months in Experiment 2 had an even more profound effect (~80% decrease) on AHN, quantified at the age of ~5.5 months [t (16) = 11.18, p < 0.001] (Figure 3, B and D). Note that in Experiment 2, the data was obtained from only eight rats in the irradiated group due to technical problems. Also note that in both experiments, the control and irradiated animals were euthanized in alternating order to maintain comparability of cell counts between groups. To summarize, irradiation of the head at both the lower and the higher dose was effective in reducing cell proliferation throughout the hippocampus.

Irradiation had no effect on electrophysiological measures of hippocampal function

To examine the effects of irradiation on hippocampal function, we recorded hippocampal electrophysiology in vivo under urethane anesthesia. The results are summarized in Figure 4. Note that data only from animals with correct electrode placement were included. The data on baseline electrophysiology is presented only from Experiment 2, as the irradiation dose was larger and the animals were irradiated younger, resulting in a more profound decrease in AHN compared to Experiment 1 (see Figure 3B). The current source density maps with averaged LFP traces superimposed (Figure 4A) indicated no difference between the irradiated (2 x 10 Gy, n = 10/9) and control rats (n = 9) in any of the oscillatory phenomena studied. The FFT grand averages lead to the same conclusion, *i.e.* no difference between the groups (see Figure 4B).

To properly address our research questions, dentate spike properties were examined further from rats in which at least 20 dentate spikes took place during the 30-min baseline recording. Note that according to current knowledge, dentate spikes should be associated with an increase in dentate granule cell membrane potential (Penttonen et al. 1997). Thus, the dentate spikes could be

sensitive to the absence of immature adult-born granule cells. However, the dentate spike occurrence rate, amplitude and slope were all similar in irradiated (n = 7) and control rats (n = 8) (one-way ANOVA: F [1, 13] = 0.00 – 0.32, p = 0.583 – 0.976). In the control group, dentate spikes took place at a rate of 2.0 ± 0.3 (M + Standard Error of Mean, SEM) per minute. In the irradiated rats, the rate was 2.1 ± 0.5. The peak amplitude and slope of the dentate spikes in the control group were 639 ± 60 μV and 62 ± 5 μV/ms, respectively. In the irradiated group the corresponding measures were 666 ± 66 μV and 63 ± 7 μV/ms. In summary, irradiation did not affect the occurrence rate of properties of dentate spikes. In terms of gamma amplitude, we detected no difference in either hilar gamma (25–80 Hz) or high gamma (80–140 Hz) amplitude between control and irradiated animals (one-way ANOVA: F[1, 17] = 0.30, p = 0.872 and F [1, 17] = 0.03, p = 0.868, respectively). Note that valid data from hilus was obtained from 18 animals. To summarize, endogenous hippocampal electrophysiology was intact even after irradiation at 2 x 10 Gy, a dose resulting in the loss of most immature adult-born new neurons in the DG.

In addition to spontaneous electrophysiology, we also studied the effects of irradiation on synaptic plasticity in the hippocampus. Again, only data from animals with correctly placed electrodes (stimulation and recording) were included. Previous research indicates that irradiation might impair long-term potentiation (LTP) in the perforant path to dentate gyrus synapse (Saxe et al. 2006; Singer et al. 2011). In Experiment 1, long-term depression at the perforant path to dentate gyrus synapse was studied. The protocol we used did not result in a consistent change in synaptic transmission in either the control (n = 6) or the experimental group (n = 7, 8.5 Gy) (see Figure 4C). There was also no difference between the groups. In Experiment 2, the long-term potentiation at the CA3-CA1 synapse was examined by applying theta-burst stimulation to the ventral hippocampal commissura and recording responses in the hippocampus. The protocol produced significant and robust LTP in both control (n = 7) and irradiated (n = 9, 2 x 10 Gy) rats (see Figure 4D). However, there was no difference between the groups. Note that as there was no indication of a group difference based on visual inspection, the statistics were not computed.

Irradiation impaired spatial recognition memory

Experiment 1

In Experiment 1, to assure that there were no underlying differences between the two groups in exploratory behavior, the animals were tested in an open field three weeks prior to irradiation, at

the age of ~3.5 months. Both animals in the control group and those in the irradiation group readily moved about in the open field arena (line crosses, control: 80 ± 10 vs. 8.5 Gy: 76 ± 9). The animals in the two groups also spent comparable time in the middle of the arena (control: 14 ± 4 s vs. 8.5 Gy: 10 ± 2 s). That is, there was no difference in the exploratory behavior between the groups prior to irradiation.

The protocol and results of further behavioral tests in Experiment 1 are summarized in Figure 5. All animals were subjected to a Context-Object Discrimination task (Figure 5A) eight weeks after the irradiation. One-way ANOVA indicated no difference in performance between the control and the irradiated animals (COD index at 1 minute: $F [1, 18] = 0.02$, $p = 0.887$) (see Figure 5D). That is, irradiation had no effect on learning or remembering which objects belong to which context.

Starting at nine weeks after irradiation, all animals were subjected to 15 daily sessions of fixed interval training (Figure 5B). There was no effect of irradiation on the performance (rm ANOVA, group x 5 blocks of 3 sessions: main effect of block: $F [4, 72] = 100.75$, $p < 0.001$; main effect of group: $F [1, 18] = 1.79$, $p = 0.198$; interaction of block and group: $F [4, 72] = 0.88$, $p = 0.483$). That is, irradiation had no effect on simple temporal learning (see Figure 5E).

In addition, all animals were subjected to an object location task using a 1-min delay (Figure 5C) twice: Once prior to irradiation, at the age of ~3.5 months and once 12 weeks after irradiation, at the age of ~7 months. Altogether eight animals in the control group and eight animals in the irradiated group successfully indicated memory for the location of the object (recognition index above 50%) prior to irradiation (Figure 5F, Time point pre), and were thus included in an analysis conducted using rm ANOVA. There was a statistically significant interaction of time point and group in the performance in the object location task: $F [1, 14] = 4.69$, $p = 0.048$. Separate rm ANOVAs for the control and irradiated groups indicated no change in the performance of the control group ($F [1, 7] = 0.00$, $p = 0.969$) but a statistically significant drop in the performance of the irradiated group ($F [1, 7] = 9.47$, $p = 0.018$). To assure that this effect was not due to a general change in exploration behavior, rm ANOVA was run on the exploration times during the initial 5-minute exploration period. There was a clear decrease in the exploratory behavior across time in both groups (main effect of time point: $F [1, 14] = 22.78$, $p < 0.001$; main effect of group: $F [1, 14] = 0.15$, $p = 0.708$; interaction of time and group: $F [1, 14] = 0.00$, $p = 0.965$) (data not shown). That is, irradiation at a dose of 8.5 Gy impaired performance in the object location task (see Figure 5F) and exploratory behavior decreased across time as the rats grew older.

Experiment 2

The behavior of the animals in Experiment 2 was tested twice: Once prior to irradiation at the age of ~3 months and eight weeks after the irradiation at the age of ~5 months (see Figure 6). The rats performed the object location task with a delay of ~65 minutes (Figure 6A and 6C). Data from animals that spent at least 5 s exploring both objects during the sample phase and the test phase were included in the analysis. This left a sample size of seven control rats and six irradiated rats. Repeated measures ANOVA revealed a significant interaction of group (Ctrl vs. 2 x 10 Gy) and time point (pre vs. post), $F [1, 11] = 4.96$, $p = 0.048$. However, post-hoc comparisons using the Bonferroni-test indicated no significant differences between the groups within each time point ($p > 0.05$) nor between time points within each group ($p > 0.05$). Further, one sample t-tests confirmed that, at the group level, rats in both groups and at both time points studied both objects at an equal rate (comparison to 50 %, $p > 0.05$). Upon more detailed inspection, 1/7 control rats studied the moved object more than the stationary object (cut-off at 65% preference) during the pre-testing and 5/7 rats did so during the post-testing. For the irradiated group the equivalent proportions were 4/6 and 3/6, respectively. To summarize, spatial recognition memory (Barker and Warburton 2011) improved in the control group.

The next day, the rats performed the episodic-like memory task (Figure 6, panels B, D and E). Data from animals that spent at least 5 s exploring both objects during both sample phases and the test phase were included in the analysis. This left a sample size of eight control rats and eight irradiated rats. Based on previous reports, the rats were expected to pay more attention to the stationary remote object (A1) and to the displaced recent object (B2) (Kart-Teke et al. 2006; Inostroza et al. 2013). Prior to irradiation, we found no difference in the exploration between the objects (A1, A2, B1, B2) or between the groups (rm ANOVA: main effect of group: $F [1, 14] = 0.09$, $p = 0.773$; main effect of object: $F [3, 42] = 1.57$, $p = 0.230$; interaction of group and object: $F [1, 42] = 1.02$, $p = 0.364$). After irradiation, we still found no difference between the groups (rm ANOVA: main effect of group: $F [1, 14] = 0.01$, $p = 0.932$) but an overall difference between the objects ($F [3, 42] = 3.63$, $p = 0.020$; interaction of group and object: $F [1, 42] = 0.67$, $p = 0.578$). However, further examination using Bonferroni-tests did not reveal significant differences in exploration between any pair of objects ($p > 0.05$). To summarize, performance in the episodic-like memory task indicated no impairment due to irradiation (Figure 6D).

To further probe performance in the episodic-like memory task, and to confirm our results, we calculated an index for both the “Where” and “When” components of the task in a manner

described in (Inostroza et al. 2013) (see Materials and Methods, Behavioral Tasks, Experiment 2, Episodic-like memory task). In one control rat, the indexes were not calculated because it did not explore the B-objects during the pre-irradiation testing. Thus, there were seven eligible rats in the control group and eight in the irradiated group. Repeated measures ANOVA indicated no difference between groups in the "Where" index ($F [1, 13] = 2.52$, $p = 0.136$) but a significant main effect of time point ($F [1, 13] = 7.19$, $p = 0.019$; interaction of group and time point: $F [1, 13] = 0.11$, $p = 0.749$) (Figure 5E). For the "When" index, rm ANOVA revealed a significant main effect of group ($F [1, 13] = 8.01$, $p = 0.014$) and a significant main effect of time point ($F [1, 13] = 9.71$, $p = 0.008$; interaction of group and time point: $F [1, 13] = 0.18$, $p = 0.675$) (Figure 6F). The performance of the rats in the current study indicated no preference for exploring the old stationary or the recently displaced object. Rather the opposite, at the age of ~5 months, especially the control rats preferred to explore the recent stationary (B1) and the old displaced objects (A2).

Discussion

Head irradiation to treat glioma is known to cause cognitive impairment in a formidable proportion of human patients. The mechanisms of how irradiation as such affects the body and the brain are not too well understood. Here, using adult male rats, we studied the effects of moderate-dose head irradiation on various measures of health with a special focus on hippocampus. Our hypothesis was that irradiation would cause systemic inflammation and alter the gut microbiota, abolish adult hippocampal neurogenesis, disrupt synaptic plasticity and endogenous neuronal activity in the hippocampus, and ultimately impair learning and memory. Somewhat surprisingly, we found no effect of irradiation on the studied health parameters or hippocampal electrophysiology. However, in agreement with previous studies, irradiation reduced AHN. At the behavioral level, irradiation impaired spatial recognition memory but overall cognitive impairment was not observed. To summarize, the effects of head irradiation were significantly lesser than expected. Therefore, based on our results in rats, it should be considered that the cognitive side-effects experienced by human cancer patients might stem from disruptions in large scale network activity across different brain structures, rather than from disruptions within a single structure such as the hippocampus that was studied here. In addition, our results suggest that the disease itself, and possibly the stress related to being ill (Randazzo and Peters, 2016), rather than the treatment as such, might explain some of the harmful symptoms experienced by cancer survivors.

Previous studies on the systemic effects of irradiation in animal models and human patients have reported that pathways leading to the production of acute pro-inflammatory cytokines can be activated as a result of radiation-induced oxidative insult and DNA damage (Gandhi and Chandna 2017; Gerassy-Vainberg et al. 2018). Radiation is known to increase, for instance, the release of cytokines TNF-α and IFNγ into the systemic circulation to generate pro-apoptotic signals. These events can further activate the transcription factor nuclear factor-κB, which, when translocated to the nucleus, induces the production of other cytokines (Gandhi and Chandna, 2017). Interestingly, irradiated rats in our current study did not differ from control rats in terms of systemic inflammation at five weeks after irradiation. In fact, the level of most cytokines probed were undetectable in our experiment both prior to and after irradiation. Only IL12 was detected yet did not differ between control and irradiated rats. Interestingly, a recent study reported that local irradiation of the lower limb muscle upregulated several systemic pro-inflammatory cytokines, but the situation normalized in 48 hours after cessation of the irradiation (Kawano et al. 2019). To

summarize, in light of previous knowledge and our current results, it seems that local irradiation of the head does not lead to long-term systemic inflammation, does not alter weight gain or compromize well-being overall.

Consistent with no effects of irradiation on the cytokines, we found only a small compositional difference in the gut microbiota of our irradiated rats compared to controls. The gut microbiota is known to influence the production of several cytokines, and conversely the cytokines can modulate the composition of the gut microbiota. It is suggested that the microbiota-cytokine interactions are stimulus-specific, cytokine-specific, and combinatorially cytokine- and stimulus-specific (Schirmer et al. 2016). While, to our knowledge, the effects of head irradiation on the gut microbiota have not been studied, the irradiation of the gut in mice has been shown to increase the abundance of *Bacteroides* (Gerassy-Vainberg, 2018), which is in agreement with our current results from head irradiation. Similarly, a study using 10 Gy whole body irradiation also found an increase in the abundance of several members of the *Bacteroidales* order in rats (Lam et al. 2012). The minor effects of head irradiation on the gut microbiota may relate to sampling time (as in the case of systemic inflammation) or to the fact that there were no changes observed in body weight due to irradiation. This is supported by the fact that cancer and cancer treatment-associated cachexia, a complex multiorgan syndrome causing significant muscle and body weight loss, has been shown to prominently alter the gut microbiota and vice versa (Bindels et al. 2018). Future studies should probe gut microbiota and systemic inflammation at different time points after head irradiation to confirm our current results.

Next, we examined AHN and *in vivo* electrophysiology of the hippocampus ~2–3 months after the head irradiation. As expected, AHN was reduced significantly by irradiation, and the cell counts clearly indicate both the reduction in overall level of AHN as a function of age (see Figure 3, compare control groups from Experiments 1 and 2) and the fact that a larger dose of irradiation reduced AHN more effectively (compare the differences between control and experimental groups in Experiments 1 and 2). However, we found no effect of irradiation, and the subsequent reduction in the number of adult-born new neurons, on either synaptic plasticity or endogenous electrophysiological activity of the hippocampus recorded *in vivo* under urethane anesthesia. These results are further discussed below.

First, previous reports have indicated a deficit in perforant path to dentate gyrus LTP but not in CA3 to CA1 LTP in animals with reduced AHN due to irradiation (Saxe et al. 2006; Snyder et al. 2001). Compatible with these earlier studies (Saxe et al. 2006; Snyder et al. 2001), we found

that also *in vivo*, under urethane anesthesia, robust LTP was elicited at the CA3-CA1 synapse in both control rats and those irradiated at 2 x 10 Gy. Compared to our current experiment conducted *in vivo* after a 20-Gy dose, in the previous experiments (Saxe et al. 2006; Snyder et al. 2001), the irradiation dose was lower and the LTP experiment was performed *in vitro*. Note that we specifically chose not to study LTP at the perforant path-dentate gyrus synapse as we assumed it would most likely have been attenuated in the irradiated rats due to the clear reduction in AHN (see Saxe et al. 2006), and the result would not have had any novelty value. We acknowledge that, on the other hand, confirming this attenuation in perforant path- dentate gyrus LTP (just as confirming the preservation of CA3-CA1 LTP) would also have been valuable from the viewpoint of reproducibility of previous results.

Second, in a separate experiment we chose to examine the effects of low-frequency stimulation of the perforant path in hope of eliciting long-term depression of responses in the dentate gyrus. Despite using a well-documented stimulation protocol, we observed no long-term depression. More importantly, we also did not find any difference in the dentate gyrus responses between control rats and rats exposed to irradiation of the head at 8.5 Gy. While this leaves the question of whether long-term depression might be compromised still open, our results do suggest no overt change in responding to weak stimulation arriving from the neocortex to the hippocampus due to head irradiation, or a reduction in AHN.

Third, upon examining spontaneous hippocampal electrophysiological activity under urethane anesthesia, we found no effect of irradiation, at either dose, on dentate spikes, i.e. hippocampal responses to endogenous input from the entorhinal cortex via the perforant path to the dentate gyrus (Bragin et al. 1995) or on the gamma oscillations generated in the dentate gyrus by the firing of principal cells orchestrated by rhythmic inhibition from GABAergic interneurons (Colgin 2016). These results are in line with our results on synaptic plasticity discussed above, but in contrast with an earlier study reporting that abolishing AHN reduced responses to perforant path stimulation and increased the amplitude of endogenous gamma-bursts at 25–80 Hz under urethane anesthesia in mice (Lacefield et al. 2012). The difference in species might explain this discrepancy. In addition, contrary to what we expected based on previous reports on the effects of abolishing AHN (Nokia et al. 2012; Park et al. 2015), we did not find any effect of irradiation on the hippocampal theta oscillations recorded under urethane anesthesia. This might be explained by the difference not only in the means of disrupting AHN (chemotherapy vs. irradiation) but also in the state of the animal, as recordings were performed in awake behaving rats in our earlier study

(Nokia et al. 2012) and in a slow-wave sleep -like state (urethane anesthesia) in the current experiment.

What is currently known about the effects of immature adult-born granule cells on the network activity of the dentate gyrus at large has been comprehensively reviewed elsewhere (see for example Tuncdemir et al., 2019). Suffice it to say that the evidence is still somewhat sparse and controversial and thus further studies are needed. In fact, many of the results concerning immature granule cell contribution to dentate gyrus activity (and behavior) seem to be context-dependent in a sense that the contribution might depend both on the state of the animal (anesthetized vs. awake relaxed vs. anxious) as well as the environmental demands (no task vs. simple foraging vs. demanding pattern separation). To summarize, according to our current results based on a limited selection of stimulation and recording protocols applied under urethane anesthesia in adult male rats, endogenous hippocampal electrophysiology related to memory consolidation off-line as well as the responses to input from the neocortex to the dentate gyrus were intact even after head irradiation -induced abolition of AHN. It is possible that differences between the control and irradiated rats would have been evident had the recordings taken place in awake state, during a cognitively demanding task such as pattern separation.

Thus, at last, we examined the effects of irradiation and abolishing AHN on learning and memory using several different behavioral tasks. Earlier findings suggest that dentate gyrus granule cells, and adult-born new neurons especially, are important for pattern separation (Clelland et al. 2009; Sahay et al. 2011; Neunuebel and Knierim 2014; Franca et al. 2017) and contextual conditioning (Saxe et al. 2006). However, we did not find any deficit in performance due to irradiation in the context-object discrimination task (8.5 Gy) or in the episodic-like memory task (2 x 10 Gy). Both of these tasks require the rats to encode and retain contextual information, and as such serve to measure pattern completion and separation. In addition to the episodic-like memory task and context-object discrimination, the performance of the irradiated (8.5 Gy) rats was comparable to that of control rats also in the fixed interval task suggesting adequate inhibitory control of behavior, an ability thought to be dependent on hippocampal function (Yin and Meck, 2014). Our current results, however, do indicate subtle decrements due to irradiation (and abolished AHN) in situations requiring simple spatial recognition memory. This is somewhat surprising taken that mostly mature granule cells, and only a small fraction of them, seem to be activated in response to these types of tasks (see Tuncdemir et al. 2019 for a review). Naturally, the discrepancies between results of previous studies and those obtained now, might be explained

by differences in the age of animals used, the delay between irradiation and behavioral testing, irradiation dose and extent, and the subsequent extent of the decrease in AHN. One must also note that the performance of even the intact control rats in our study was very variable in the spatial tasks relying on effective object exploration: It would seem that in many cases the animals paid minimal attention to the task at hand. In this regard, tasks based on direct motivation for immediate behavior with either appetitive or aversive stimulation might be better suited for observing differences between the performance of groups of rats. Task that might be useful in further experiments include pattern separation tasks performed in a maze (Clelland et al. 2009) and simple contextual fear conditioning (Sahay et al. 2011; Saxe et al. 2006; Winocur et al. 2006). To summarize our current findings regarding behavior, irradiation and subsequent decline in AHN did not produce an impairment in the tests employed in this study in adult male rats.

Before drawing further conclusion, there are some aspects of our current study that should be considered further. First, for cancer patients, irradiation is usually performed several times but using smaller doses at a time, for example, a total of 50 Gy in 2 Gy doses over the course of 5 weeks, while here we irradiated rats only once or twice using a rather high dose. Thus, some of the harmful side effects evident in humans but not detected in our rat study might only develop as a result of repetitive irradiation over time. Second, humans are not rats, so the results of our current study cannot be directly attributed to the human brain and behavior. For example, the presence of AHN in the human brain is still under debate (see for example Lucassen et al., 2020; Petrik and Encinas, 2019). However, basic mechanisms of neural plasticity thought to underlie learning and memory are similar in both rats and humans, and thus the fact that hippocampal synaptic plasticity was not affected by irradiation in rats here, even after a dose 20 Gy, suggests it should be maintained rather intact also in humans receiving irradiation of the head. Third, even though we used two groups of adult rats of different ages in the current experiment, and glioma incidence and mortality is highest among rather young patients, it would have been good to include a group that would have been old enough (> 2 years; see Sengupta, 2013) to represent a typical cancer patient, i.e. a human over 65 years of age (Miller et al. 2019). When planning further studies, the aforementioned should be taken into consideration.

Conclusion

Our current results indicate very limited effects of head irradiation on overall health in rats. However, as expected, irradiation lead to a reduction in adult hippocampal neurogenesis. In terms of the functional significance of adult hippocampal neurogenesis, our current findings hint the new neurons play only a limited role in learning: Irradiated rats performed similar to control rats in most behavioral tasks although they were impaired in a task measuring spatial memory. Further, somewhat surprisingly, our current results indicated no differences between the irradiated and the control group in spontaneous hippocampal electrophysiology, recorded under urethane anesthesia, or in the tests of hippocampal synaptic plasticity applied in our study. To conclude, it might be that the cognitive deficits experienced by human cancer patients are brought about by the combined biological, physiological and psychosocial effects of the disease itself and its repeated treatment, and not just irradiation. Further studies will be needed to corroborate our results.

Acknowledgements

We thank Henriikka Huhtamäki, Eveliina Pöllänen, Hanna Tammisto, Aino Pirkkala and Tiina Pirttimäki for their contribution to data acquisition and analysis, and Arto Lipponen, Lauri Kantola, Hanne Tähti, Mervi Matero, Eliisa Kiukkanen, and Lauri Viljanto for technical help. We also thank Mikko Rossi and Jukka Jaatinen for making the irradiation happen. This work was supported by the Academy of Finland (275954, 286384 and 313334 to M.S.N., 316966 to M.P., and 308042 to S.P.). The foundation of Jenny and Antti Wihuri and the Central Finland Regional fund of the Finnish Cultural Foundation are acknowledged for their personal grants to S.L.

Conflict of Interest Statement

The authors have no conflict of interest to declare.

Author Contributions

All authors together designed the study and analyses. SL, TW, EM, MN and SP acquired the data. SL, EM, MN and SP analyzed the data. MN and SL made the figures. MN and SL were in charge of and all authors contributed to writing the manuscript.

Data Accessibility Statement

Data is accessible upon request from corresponding author.

Abbreviations

ANOVA = analysis of variance; AHN = adult hippocampal neurogenesis; COD = context-object discrimination; CSD = current source density; DCX = doublecortin; FI = fixed interval; FFT = Fast Fourier Transform; IL = interleukin; IFNγ = interferon-γ; LFP = local-field potential; LTP = long-term potentiation; SPW-Rs = sharp-wave ripples; TNFα = tumor necrosis factor-α; vHC = ventral hippocampal commissure.

References

Anacker C, Luna VM, Stevens GS, Millette A, Shores R, Jimenez JC, Chen B, Hen R. 2018. Hippocampal neurogenesis confers stress resilience by inhibiting the ventral dentate gyrus. Nature. 559:98-102.

Barker GR, Warburton EC. 2011. When is the hippocampus involved in recognition memory? J Neurosci. 31:10721-10731.

Bindels LB, Neyrinck AM, Loumaye A, Catry E, Walgrave H, Cherbuy C, … , Delzenne NM. 2018. Increased gut permeability in cancer cachexia:mechanisms and clinical relevance. Oncotarget. 9:18224-18238.

Bonaz B, Bazin T, Pellissier S. 2018. The vagus nerve at the interface of the microbiota-gut-brain axis. Front Neurosci. 12:49.

Bragin A, Jando G, Nadasdy Z, van Landeghem M, Buzsaki G. 1995. Dentate EEG spikes and associated interneuronal population bursts in the hippocampal hilar region of the rat. J Neurophysiol. 73:1691-1705.

Burghardt NS, Park EH, Hen R, Fenton AA. 2012. Adult-born hippocampal neurons promote cognitive flexibility in mice. Hippocampus. 22:1795-1808.

Buzsáki G. 2002. Theta oscillations in the hippocampus. Neuron. 33:325-340.

Buzsáki G. 2015. Hippocampal sharp wave-ripple: A cognitive biomarker for episodic memory and planning. Hippocampus. 25:1073-188.

Clelland CD, Choi M, Romberg C, Clemenson GD Jr, Fragniere A, Tyers P, … , Bussey TJ. 2009. A functional role for adult hippocampal neurogenesis in spatial pattern separation. Science. 325:210-213.

Colgin LL. 2016. Rhythms of the hippocampal network. Nat Rev Neurosci. 17:239-249.

Cryan JF, O'Riordan KJ, Sandhu K, Peterson V, Dinan TG. 2020. The gut microbiome in neurological disorders. Lancet Neurol. 19:179-194.

Czerniawski J, Miyashita T, Lewandowski G, Guzowski JF. 2015. Systemic lipopolysaccharide administration impairs retrieval of context-object discrimination, but not spatial, memory: Evidence for selective disruption of specific hippocampus-dependent memory functions during acute neuroinflammation. Brain Behav Immun. 44:159-166.

Franca TFA, Bitencourt AM, Maximilla NR, Barros DM, Monserrat JM. 2017. Hippocampal neurogenesis and pattern separation: A meta-analysis of behavioral data. Hippocampus. 27:937-950.

Gandhi S, Chandna S. 2017. Radiation-induced inflammatory cascade and its reverberating crosstalks as potential cause of post-radiotherapy second malignancies. Cancer Metastasis Rev. 36:375-393.

Gerassy-Vainberg S, Blatt A, Danin-Poleg Y, Gershovich K, Sabo E, Nevelsky A, … , Chowers Y. 2018. Radiation induces proinflammatory dysbiosis: transmission of inflammatory susceptibility by host cytokine induction. Gut. 67:97-107.

Gondi V, Hermann BP, Mehta MP, Tomé WA. 2012. Hippocampal dosimetry predicts neurocognitive function impairment after fractionated stereotactic radiotherapy for benign or low-grade adult brain tumors. Int J Radiat Oncol Biol Phys. 83:e487-e493.

Headley DB, Kanta V, Pare D. 2017. Intra- and interregional cortical interactions related to sharp-wave ripples and dentate spikes. J Neurophysiol. 117:556-565.

Ikrar T, Guo N, He K, Besnard A, Levinson S, Hill A, … , Sahay A. 2013. Adult neurogenesis modifies excitability of the dentate gyrus. Front Neural Circuits. 7:204.

Inostroza M, Brotons-Mas JR, Laurent F, Cid E, Menendez de la Prida, L. 2013. Specific impairment of "what-where-when" episodic-like memory in experimental models of temporal lobe epilepsy. J Neurosci. 33:17749-17762.

Inostroza M, Cid E, Brotons-Mas J, Gal B, Aivar P, Uzcategui YG, Sandi C, Menendez de la Prida, L. 2011. Hippocampal-dependent spatial memory in the water maze is preserved in an experimental model of temporal lobe epilepsy in rats. PLoS One. 6:e22372.

Janelsins MC, Heckler CE, Peppone LJ, Kamen C, Mustian KM, ..., Morrow GR. 2017. Cognitive complaints in survivors of breast cancer after chemotherapy compared with age-matched controls: An analysis from a nationwide, multicenter, prospective longitudinal study. J Clin Oncol. 35:506-514.

Janelsins MC, Kohli S, Mohile SG, Usuki K, Ahles TA, Morrow GR. 2011. An update on cancer- and chemotherapy-related cognitive dysfunction: current status. Semin Oncol. 38:431-438.

Kart-Teke E, De Souza Silva, M A, Huston JP, Dere E. 2006. Wistar rats show episodic-like memory for unique experiences. Neurobiol Learn Mem. 85:173-182.

Kawano Y, Byun DK, Frisch BJ, Kawano H, LaMere MW, Johnston CJ, Williams JP, Calvi LM. 2019. Local Irradiation Induces Systemic Inflammatory Response and Alteration of the Hematopoietic Stem Cell Niche. Blood 134 (Supplement_1): 1213.

Knierim JJ, Neunuebel JP. 2016. Tracking the flow of hippocampal computation: Pattern separation, pattern completion, and attractor dynamics. Neurobiol Learn Mem. 129:38-49.

Lacefield CO, Itskov V, Reardon T, Hen R, Gordon JA. 2012. Effects of adult-generated granule cells on coordinated network activity in the dentate gyrus. Hippocampus. 22:106-116.

Lam V, Moulder JE, Salzman NH, Dubinsky EA, Andersen GL, Baker JE. 2012. Intestinal microbiota as novel biomarkers of prior radiation exposure. Radiat Res. 177:573-83

Lawrie TA, Gillespie D, Dowswell T, Evans J, Erridge S, Vale L, Kernohan A, Grant R. 2019. Long-term neurocognitive and other side effects of radiotherapy, with or without chemotherapy, for glioma. Cochrane Database Syst Rev. 8:CD013047.

Lensu S, Waselius T, Penttonen M, Nokia MS. 2019. Dentate spikes and learning: disrupting hippocampal function during memory consolidation can improve pattern separation. J Neurophysiol. 121:131-139.

Lin C, Chen C, Chiang H, Liou J, Chang C, Lu T, …, Wu M. 2019. Altered gut microbiota and inflammatory cytokine responses in patients with Parkinson's disease. J Neuroinflammation. 16:129.

Lucassen PJ, Fitzsimons CP, Salta E, Maletic-Savatic 2020. M. Adult neurogenesis, human after all (again): Classic, optimized, and future approaches. Behav Brain Res. 381:112458.

MacDonald CJ, Lepage KQ, Eden UT, Eichenbaum H. 2011. Hippocampal "time cells" bridge the gap in memory for discontiguous events. Neuron. 71:737-749.

Mau W, Sullivan DW, Kinsky NR, Hasselmo ME, Howard MW, Eichenbaum H. 2018. The same hippocampal CA1 population simultaneously codes temporal information over multiple timescales. Current Biology. 28:1499-1508.e4.

Miller KD, Nogueira L, Mariotto AB, et al. 2019. Cancer treatment and survivorship statistics, 2019. CA Cancer J Clin. 69(5):363-385.

Miller LN, Weiss C, Disterhoft JF. 2019. Genetic ablation of neural progenitor cells impairs acquisition of trace eyeblink conditioning. eNeuro. 6:10.

Miller SM, Sahay A. 2019. Functions of adult-born neurons in hippocampal memory interference and indexing. Nat Neurosci. 22:1565-1575.

Monje ML, Mizumatsu S, Fike JR, Palmer TD. 2002. Irradiation induces neural precursor-cell dysfunction. Nat Med. 8:955-962.

Mumby DG, Gaskin S, Glenn MJ, Schramek TE, Lehmann H. 2002. Hippocampal damage and exploratory preferences in rats: memory for objects, places, and contexts. Learn Mem. 9:49-57.

Neunuebel JP, Knierim JJ. 2014. CA3 retrieves coherent representations from degraded input: direct evidence for CA3 pattern completion and dentate gyrus pattern separation. Neuron. 81:416-427.

Nokia MS, Gureviciene I, Waselius T, Tanila H, Penttonen M. 2017. Hippocampal electrical stimulation disrupts associative learning when targeted at dentate spikes. J Physiol. 595:4961-4971.

Nokia MS, Lensu S, Ahtiainen JP, Johansson PP, Koch LG, Britton SL, Kainulainen H. 2016. Physical exercise increases adult hippocampal neurogenesis in male rats provided it is aerobic and sustained. J Physiol. 594:1855-73.

Nokia MS, Anderson ML, Shors TJ. 2012. Chemotherapy disrupts learning, neurogenesis and theta activity in the adult brain. Eur J Neurosci. 36:3521-30.

O'Keefe J, Dostrovsky J. 1971. The hippocampus as a spatial map. Preliminary evidence from unit activity in the freely-moving rat. Brain Res. 34:171-175.

Park EH, Burghardt NS, Dvorak D, Hen R, Fenton AA. 2015. Experience-dependent regulation of dentate gyrus excitability by adult-born granule cells. J Neurosci. 35:11656-11666.

Pastalkova E, Itskov V, Amarasingham A, Buzsaki G. 2008. Internally generated cell assembly sequences in the rat hippocampus. Science. 321:1322-1327.

Paxinos G. WC. 1998. The rat brain in stereotaxic coordinates. San Diego, California, USA: Academic Press, Inc. 256 p.

Penttonen M, Kamondi A, Sik A, Acsady L, Buzsaki G. 1997. Feed-forward and feed-back activation of the dentate gyrus in vivo during dentate spikes and sharp wave bursts. Hippocampus. 7:437-450.

Petrik D, Encinas JM. 2019. Perspective: Of Mice and Men - How Widespread Is Adult Neurogenesis?. Front Neurosci. 13:923.

Randazzo D, Peters KB. 2016. Psychosocial distress and its effects on the health-related quality of life of primary brain tumor patients. CNS Oncol. 5:241-249.

Sahay A, Scobie KN, Hill AS, O'Carroll CM, Kheirbek MA, Burghardt NS, …, Hen R. 2011. Increasing adult hippocampal neurogenesis is sufficient to improve pattern separation. Nature. 472:466-470.

Saxe MD, Battaglia F, Wang JW, Malleret G, David DJ, Monckton JE, …, Drew MR. 2006. Ablation of hippocampal neurogenesis impairs contextual fear conditioning and synaptic plasticity in the dentate gyrus. Proc Natl Acad Sci U S A 103:17501-17506.

Schirmer M, Smeekens SP, Vlamakis H, Jaeger M, Oosting M, Franzosa EA, …, Xavier RJ. 2016. Linking the human gut microbiome to inflammatory cytokine production capacity. Cell 167:1125-1136.e8.

Scoville WB, Milner B. 1957. Loss of recent memory after bilateral hippocampal lesions. Journal of Neurology, Neurosurgery, and Psychiatry. 20:11-21.

Sengupta P. 2013. The Laboratory Rat: Relating Its Age With Human's. Int J Prev Med. 4(6):624-630.

Seo D, Carillo MA, Chih-Hsiung Lim S, Tanaka KF, Drew MR. 2015. Adult hippocampal neurogenesis modulates fear learning through associative and nonassociative mechanisms. J Neurosci. 35:11330-11345.

Serbanescu MA, Mathena RP, Xu J, Santiago-Rodriguez T, Hartsell TL, Cano RJ, Mintz CD. 2019. General anesthesia alters the diversity and composition of the intestinal microbiota in mice. Anesth Analg. 129:e126-e129.

Shors TJ, Miesegaes G, Beylin A, Zhao M, Rydel T, Gould E. 2001. Neurogenesis in the adult is involved in the formation of trace memories. Nature. 410:372-376.

Singer BH, Gamelli AE, Fuller CL, Temme SJ, Parent JM, Murphy GG. 2011. Compensatory network changes in the dentate gyrus restore long-term potentiation following ablation of neurogenesis in young-adult mice. Proc Natl Acad Sci U S A. 108:5437-5442.

Smith LK, Wissel EF. 2019. Microbes and the mind: How bacteria shape affect, neurological processes, cognition, social relationships, development, and pathology. Perspect Psychol Sci. 14:397-418.

Snyder JS, Kee N, Wojtowicz JM. 2001. Effects of adult neurogenesis on synaptic plasticity in the rat dentate gyrus. J Neurophysiol. 85:2423-31.

Toda T, Gage FH. 2018. Review: adult neurogenesis contributes to hippocampal plasticity. Cell Tissue Res. 373:693-709.

Touchefeu Y, Montassier E, Nieman K, Gastinne T, Potel G, Bruley des Varannes S, …, de La Cochetiere MF. 2014. Systematic review: the role of the gut microbiota in chemotherapy- or radiation-induced gastrointestinal mucositis - current evidence and potential clinical applications. Aliment Pharmacol Ther. 40:409-421.

Trotti A, Bellm LA, Epstein JB, Frame D, Fuchs HJ, Gwede CK, …, Zilberberg MD. 2003. Mucositis incidence, severity and associated outcomes in patients with head and neck cancer receiving radiotherapy with or without chemotherapy: a systematic literature review. Radiother Oncol. 66:253-262.

Tuncdemir SN, Lacefield CO, Hen R. 2019. Contributions of adult neurogenesis to dentate gyrus network activity and computations. Behav Brain Res. 374:112112.

Winocur G, Wojtowicz JM, Sekeres M, Snyder JS, Wang S. 2006. Inhibition of neurogenesis interferes with hippocampus-dependent memory function. Hippocampus. 16:296-304.

Winocur G, Wojtowicz JM, Tannock IF. 2015. Memory loss in chemotherapy-treated rats is exacerbated in high-interference conditions and related to suppression of hippocampal neurogenesis. Behav Brain Res. 281:239-244.

Yin B, Meck WH. 2014. Comparison of interval timing behaviour in mice following dorsal or ventral hippocampal lesions with mice having delta-opioid receptor gene deletion. Philos Trans R Soc Lond B Biol Sci. 369:20120466.

Zhuo J, Tseng H, Desai M, Bucklin ME, Mohammed AI, Robinson NT, …, Han X. 2016. Young adult born neurons enhance hippocampal dependent performance via influences on bilateral networks. Elife. 5:e22429.

Figure captions

Figure 1. Effects of irradiation of the head were studied in two experiments using adult male Sprague-Dawley rats. A) Experiment 1. Animals in the experimental group were exposed to irradiation at 8.5 Gy while control animals (Ctrl) were not. B) Experiment 2. Animals in the experimental group were exposed twice to irradiation at 10 Gy while control animals (Ctrl) were not. IHC = immunohistochemistry. In Experiment 2, systemic inflammation was analyzed from blood samples collected two weeks prior to irradiation and five weeks after irradiation. In addition, gut microbiota composition was examined from feces collected five weeks after irradiation. C) There was no difference in bodyweights between irradiated and control animals in either of the experiments. Data from Experiment 1 is plotted in black and that from Experiment 2 in grey. Vertical lines indicate SEM. Arrows mark the timing of the irradiation.

Figure 2. Irradiation at 2 x 10 Gy targeted to the head had no effect on overall wellbeing of adult male rats. A) Inflammatory markers were analyzed from serum drawn two weeks before and five weeks after irradiation. Of all markers only IL12 was reliably detected and irradiation did not increase its level. B) Gut microbiota alpha-diversity measured with Shannon index was very similar in irradiated and control animals five weeks after irradiation. C and D) The only statistically significant difference in the gut microbiota composition was that the abundance of *Bacteroides* belonging to the family Bacteroidaceae was higher in irradiated rats than in controls. E) Principal component (PC) analysis of gut microbiota beta-diversity revealed no differences in the Bray Curtis (i) or Weighted unifrac (ii) distances between the groups. F) As mentioned, overall the gut microbiota composition was similar in control and irradiated rats at the level of phylum (i), family (ii) and genus (iii). Asterisk refers to statistically significant effect: * = $p < 0.050$.

Figure 3. Irradiation of the head reduced adult hippocampal neurogenesis (AHN). Adult hippocampal neurogenesis was quantified by counting the number of doublecortin (DCX) positive cells in the dentate gyrus (brown cells in C and D). Cells were counted and images taken with Leica VT1000 microscope. Photos in C and D were taken at 10x and at 100x magnification. The calibration bars (100 μm) are shown in the upper panel of Fig. 3C.

Both a single dose at 8.5 Gy at the age of 18 weeks (Experiment 1, A and C) and a double dose at 10 Gy at the age of 12 weeks (Experiment 2, B and D) effectively reduced the number of immature neurons in the hippocampus. Asterisks refer to statistically significant effect: *** = $p < 0.001$. Note that the number of DCX+ cells in the older control animals (Experiment 1, A and C)

is smaller than that in younger control animals (Experiment 2, B and D) reflecting the age-related decline in AHN.

Figure 4. Spontaneous oscillations or synaptic plasticity in the hippocampus, recorded under urethane anesthesia, were not affected by irradiation. A) Current-source density (CSD) maps and local-field potential average traces from two representative animals from Experiment 2 (i: control, ii: 2 x 10 Gy). Sharp-wave ripples (SPW-R), theta (3–8 Hz), gamma (25–80 Hz and 80–140 Hz) and dentate spikes (DS) all were intact also in irradiated rats. Horizontal scale bars equal to 100 ms. Vertical scale bar equals to 500 μV and refers to the local-field potentials. CSD map colors indicate source and sink, and are in the same scale for all panels. B) FFTs calculated for data recorded during the baseline in Experiment 2 also revealed no effect of irradiation. Note the prominent theta in the molecular layer and gamma in hilus. Solid lines mark grand averages and dottes lines indicate the standard error of mean. C) In Experiment 1, low-frequency stimulation (LFS) of the perforant path (PP) resulted in similar synaptic transmission to the dentate gyrus (DG) in both control and irradiated rats. D) In Experiment 2, theta-burst stimulation (TBS) of the ventral hippocampal commissure (vHC) resulted in similar synaptic transmission to the CA1 in both control and irradiated rats. Note the prominent long-term potentiation in both. In panels C and D, the solid horizontal reference line marks the level of responses to stimulation during baseline (100%).

Figure 5. Irradiation at 8.5 Gy impaired spatial recognition memory. A and D) Irradiated rats (8.5 Gy, n = 10) did not differ from control rats (Ctrl, n = 10) in a context-object discrimination (COD) task. B and E) Irradiation also had no effect on learning a fixed interval task with a 143 s interval. C and F) However, irradiation impaired performance in a simple object location task with a delay of just one minute. Asterisk refers to statistically significant effect: * = $p < 0.050$.

Figure 6. Irradiation at 2x 10 Gy impaired spatial recognition memory. A and C) Irradiation impaired performance in the object location task with a delay of 65 min. B and D) Performance in the episodic-like memory task was similar in both control and irradiated. Rats seemed to not distinguish between objects before irradiation. After irradiation, rats seemed to prefer the old displaced (A2) and the recent stationary (B1) objects. E and F) This was also evident when the "Where" and "When" indexes based on (Inostroza et al. 2013) were examined. These indexes are close to zero if the rat shows no preference and explores all objects at a chance level. If the index is positive, the rat preferred to explore the recently displaced object (B2, "Where") or the old

stationary object (A1, “When”). If the index is negative, the rat preferred to explore the recent stationary object (B1).

Asterisks refer to statistically significant effects: * = $p < 0.05$.

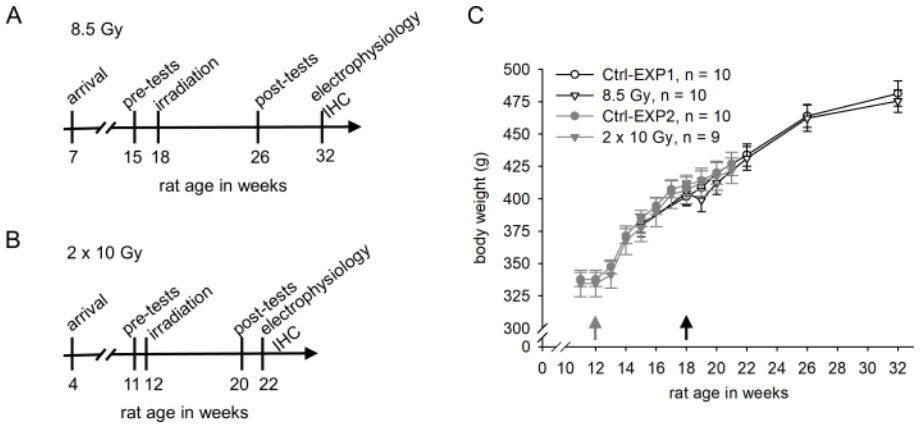

ejn_15102_f1.tif

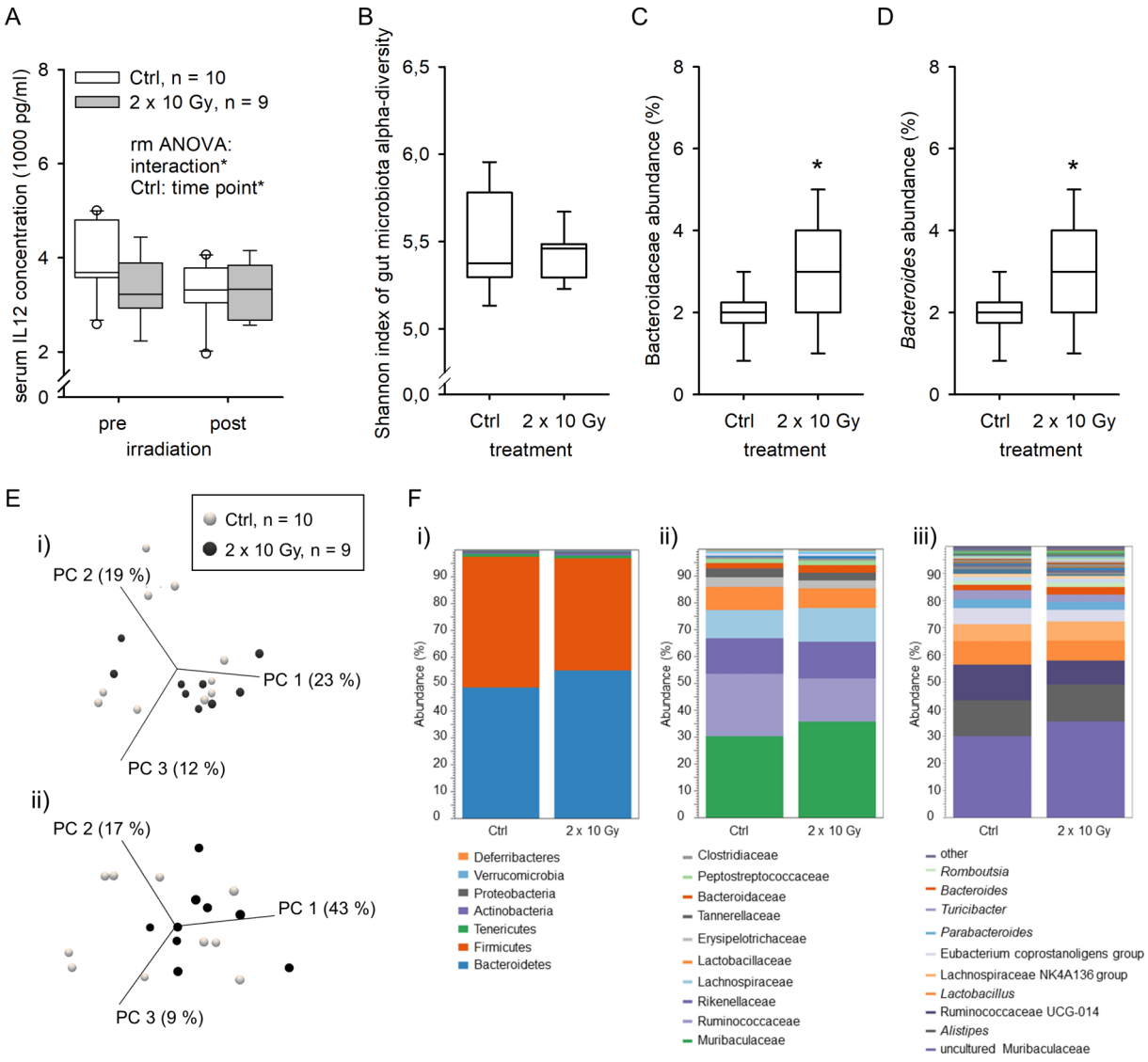

ejn_15102_f2.tif

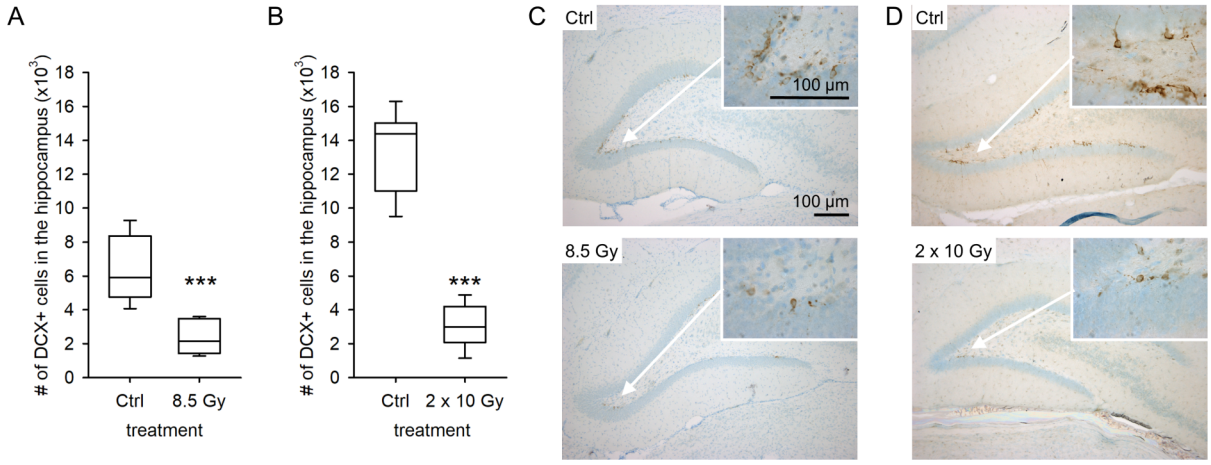

ejn_15102_f3.tif

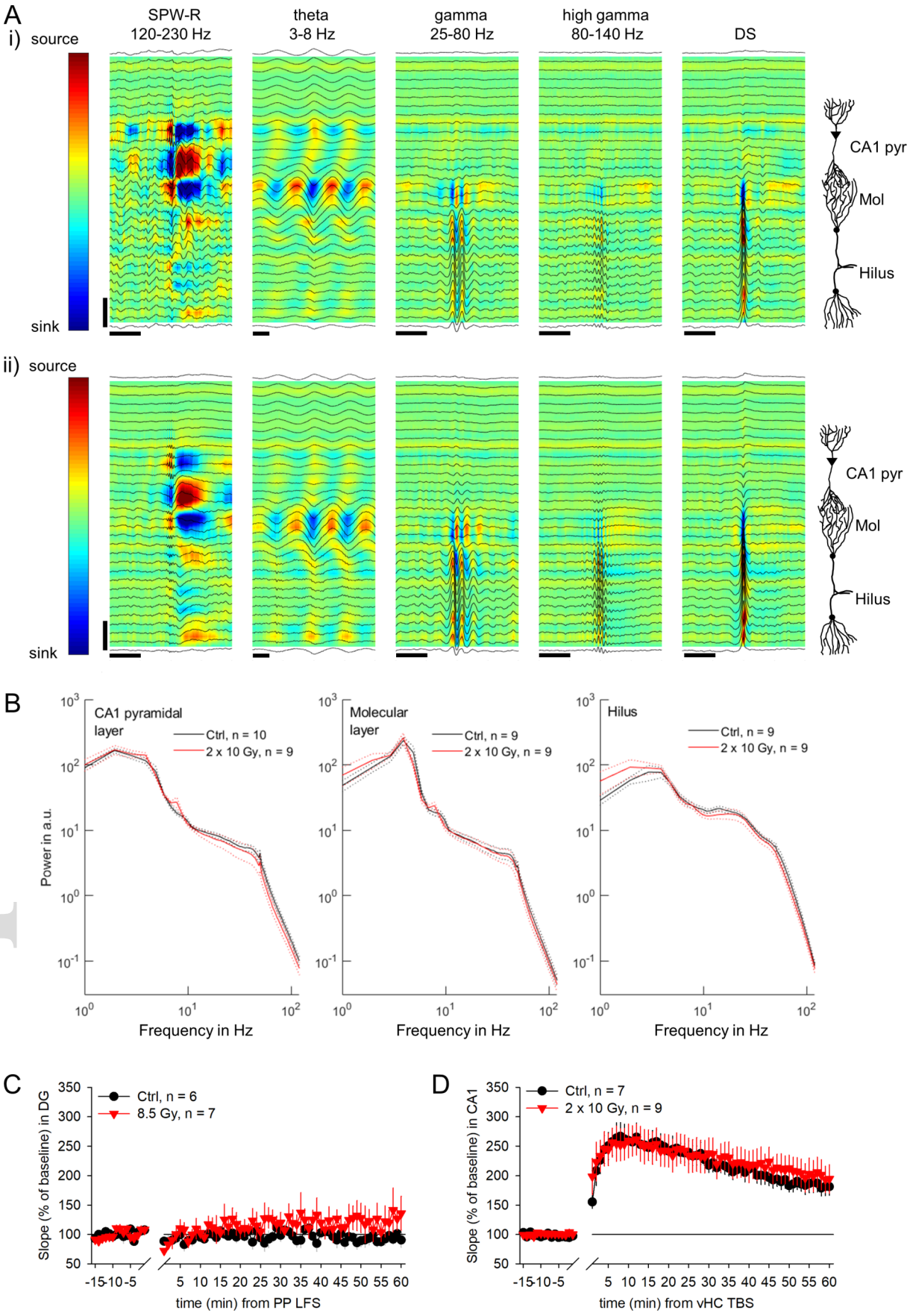

ejn_15102_f4.tif

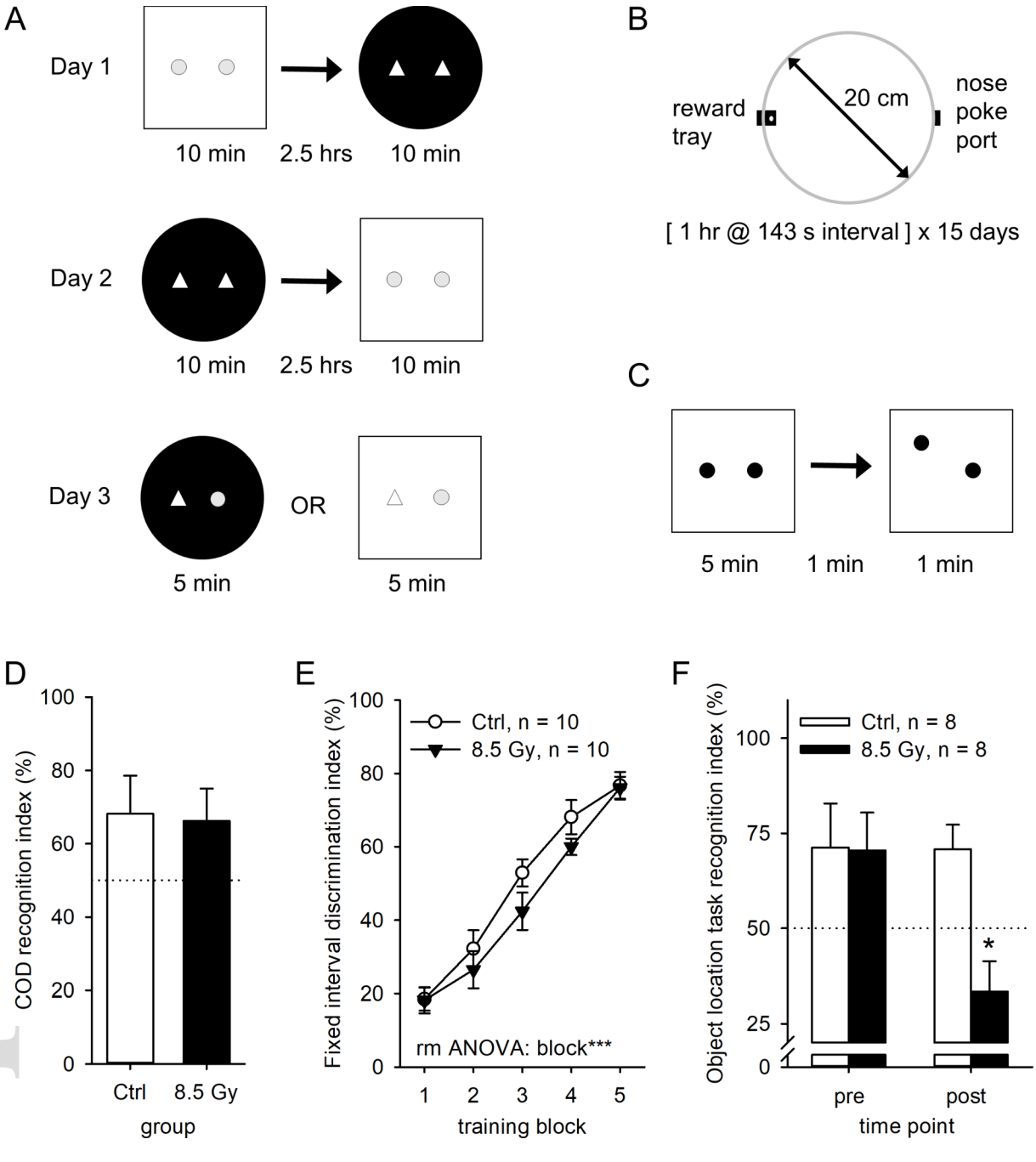

ejn_15102_f5.tif

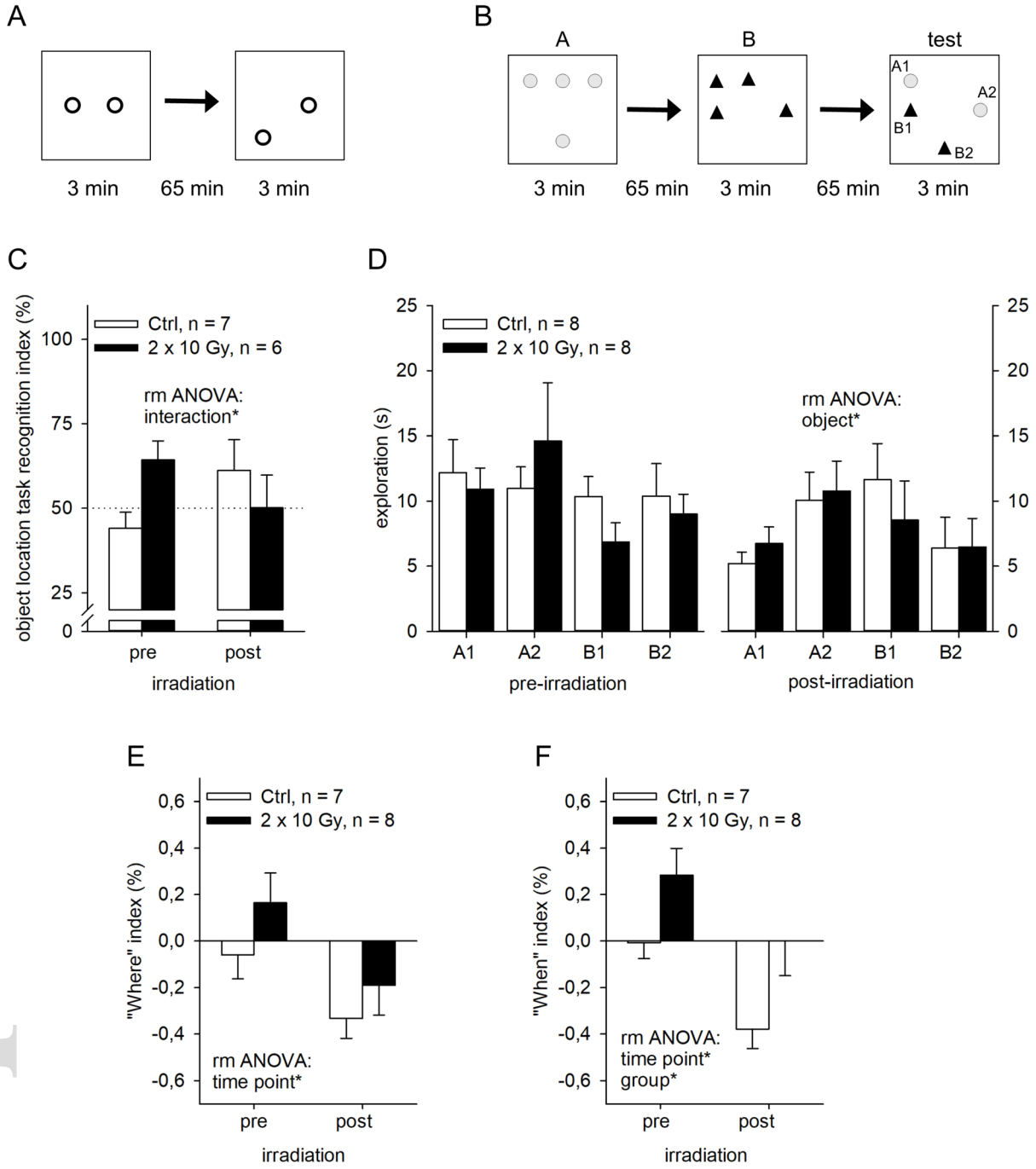

ejn_15102_f6.tif